TREBALL DE FI DE GRAU

Grau de Bioquímica i Biologia Molecular

Water Deficit and Osmotic Stress Induce Oxidative Stress and Affects Gluthatione Homeotasis in Pisum sativum L.

Joana Borobia Roca

Scientific director:
Dr. Marek Petřivalský
Department of Biochemistry, Faculty of Science, Palacký University in Olomouc, Olomouc, Czech Republic.

Palacký University
Olomouc

Academic tutor:
Dr. Juan Bautista Fernández Larrea
Departament de Bioquímica i Biotecnologia, Universitat Rovira i Virgili, Tarragona, Spain
.

UNIVERSITAT ROVIRA i VIRGILI

Universitat Rovira i Virgili
Tarragona
July 2024

INDEX

ACKNOWLEDGEMENTS

This work is part of a large-scale multidisciplinary project named TowArds Next GENeration Crops (TANGENC), which is funded by a grant from the European Union and administered by the Ministry of Education of the Czech Republic. The work presented in the TFG is part of a research project.

I would like to thank the Department of Biochemistry at Palacký University, especially Marek Petřivalský, for giving me the opportunity to be part of his research team during these months.

Additionally, I would like to thank my family for giving me the opportunity to complete my final year of university studies, and finally, my friends for accompanying me on this journey.

1. ABSTRACT

Drought and saline stress are prevalent environmental issues that severely constrain crop growth, affecting nearly all aspects of plant functioning. Stress induced by these factors is often accompanied by oxidative stress, resulting from an imbalance between the production of reactive oxygen species (ROS) and the activity of antioxidant defenses.

The aim of this study was to investigate how stress arising from water deficit and osmotic stress influences the antioxidant mechanisms associated with glutathione in *Pisum sativum L.*

To achieve these goals, we first administered two polyethylene glycol (PEG) solutions with concentrations of 10% and 20% to the roots of *Pisum sativum L* cultures during the early stages of growth over one week. We then assessed the levels of reduced and oxidized glutathione (GSH and GSSG respectively), the activity of the enzyme glutathione reductase (GR), a limiting factor in gluthatione sinthesys, and various other parameters indicative of oxidative stress, such as lipid peroxidation, S-nitrosothiol content and concentrations of malondialdehyde (MDA) in the roots of the treated plants. Our finding revealed the onset of oxidative stress in the roots of *P. sativum*, when treated with 10% and 20% PEG, as evidenced by increased concentrations of MDA and elevated GR activity in the roots. However, results regarding the GSH/GSSG ratio were not conclusive.

ABBREVIATIONS

γ-ECS, γ-glutamylcysteine synthetase;

APX, ascorbate peroxidase;

BSA, bovine serum albumin;

Cys, cysteine;

DAR, dehydroascorbate reductase;

GR, glutathione reductase;

GSH, reduced glutathione;

GSH-S, glutathione synthetase;

GSNO, nitrosoglutathione;

GSNOR, S-nitrosoglutathione reductase;

GSSG, oxidized glutathione;

LP, lipid peroxidation;

MBB, monobromobimane;

MDA, malondialdehyde;

MDAR, monodehydroascorbate reductase;

NED, N-(1-naphthylethylene)diamine;

NO, nitric oxide;

OEC, oxygen-evolving complex;

PAR, photosyntht ically active radiation;

PEG, polyethylene glycol;

PSI, photosystem I;

PSII, photosystem II;

PUFAs, Polyunsaturated fatty acids;

ROS, reactive oxygen species;

RNS, reactive nitrogen species;

RuBisCo, ribulose-1,5-biphosphate carboxylase/oxygenase;

SD, standard deviation;

SNO, S-nitrosothiol;

TBA, thiobarbituric acid;

TBARS, thiobarbituric acid-reactive substances.

2. INTRODUCTION

Currently, climate change is one of the most evident and significant problems on our planet. Among its numerous consequences are droughts and soil degradation, which pose a serious threat to crops. One of the main causes of soil degradation in the world is salt stress and, in fact, it is estimated that more than 6% of land areas and 20% of irrigated areas in the world are affected by salinization (Tokarz et al., 2021). Furthermore, approximately 60% of cultivated fields are already impacted by droughts at present (Soudek et al., 2024).

It is worth mentioning that the Czech Republic is situated among the countries where drought has become a relevant concern and a key topic of debate. Between the years 2014 and 2020, the most severe drought in the last 500 years occurred, distinguished by its extended duration and elevated temperatures compared to previous occurrences (Soudek et al., 2024).

In the future, this problem is expected to become even more intensified. Over the last 70 years, there has been an exponential growth in the global population, which is expected to increase by an additional 2 billion in the next 30 years (Soudek et al., 2024). Consequently, both food production and the expansion of arable land will need to increase. These areas will require intensive irrigation due to insufficient precipitation and/or saline soils. Additionally, the increase in freshwater deficit will require the use of seawater for crop irrigation. Therefore, salinity issues are expected to intensify further (Tokarz et al., 2021).

Crops such as wheat, rice, and legumes will assume a critical role in ensuring global food security. Nevertheless, this security will be threatened by soil degradation, severe droughts, and salinity, predominantly attributed to the extreme environmental conditions induced by climate change (Soudek et al., 2024).

As previously mentioned, salt stress and drought are very common environmental issues. Moreover, they represent some of the most significant abiotic stresses and are major limiting factors in crop breeding, given their broad impact on various plant functions (Hernández et al., 1999).

In general, plants exposed to abiotic stresses that lead to dehydration, such as drought or salinity, exhibit very similar responses. Primarily, they must cope with osmotic stress, induced by the reduction in soil water potential, and ionic stress, caused by the accumulation of Na^+ and Cl^- ions in toxic amounts. As a consequence of the reduction in soil water potential, there is insufficient water available for the plants, which in turn causes a decrease in cellular water content and a loss of turgor. Although the reduction in cell volume is temporary, it results in a limitation of the plant's growth and development (Tokarz et al., 2021). Consequently, both drought and salinity or osmotic stress can manifest as water stress (Popović et al., 2017).

When facing water stress, as mentioned earlier, plant growth is inhibited, and there is a loss of turgor. Additionally, wilting of the organs occurs along with changes in carbon and nitrogen metabolism (Lahuta et al., 2022).

The primary defense mechanism of plants in response to water deficit involves the closing of stomata and the reduction of transpiration, which leads to changes in photosynthetic pathways and a decrease in the photosynthesis process (Lahuta et al., 2022). Moreover, there is also ionic regulation through the uptake, transport, accumulation or exclusion, and selective compartmentalization of ions at the cellular or whole-plant levels. This aims to accumulate osmotically active inorganic ions and other metabolites in the root and leaf cells. This process is

coupled with the synthesis of osmoprotectants and the induction of antioxidant defense mechanisms (Piterková et al., 2012).

As a result, the osmotic potential of the cells increases, which inhibits water loss and allows the roots to continue absorbing water from the soil (Lahuta et al., 2022).

In addition to osmotic and water stress, it has also been noted that plants subjected to abiotic stresses must deal with ionic stress caused by the accumulation of ions in toxic amounts. Plants have the ability to store a certain number of harmful ions in the vacuole, but an excess can limit the vacuole's compartmentalization capacity, leading to their accumulation in the cytoplasm. This, in turn, adversely affects cellular metabolism.

One consequence of water stress is alterations in the photosynthetic pathways, resulting in a decreased efficiency of photosynthesis. Similarly, under ionic stress, plants undergo comparable changes as the ions that accumulate in the roots can freely move with the transpiration stream and reach the leaves, where they can negatively impact photosynthesis.

Photosynthetic efficiency depends on the sequence of metabolic processes occurring during the light and dark phases, the activity of enzymes involved in carbon assimilation, the structure of the photosynthetic apparatus, and the transport of intermediates between cellular compartments. Ionic stress interferes with these processes through both direct and indirect mechanisms.

Harmful ions can accumulate in the chloroplasts, causing a direct toxic effect on photosynthetic processes by degrading pigments, reducing chlorophyll concentrations in the leaves, and disrupting the thylakoid membrane structure. Furthermore, this leads to the destabilization of the protein complexes in the electron transport chain, including Photosystem II (PSII) containing the oxygen-evolving complex (OEC), photosystem I (PSI), the cytochrome b6f complex, and ATP synthase.

Indirectly, ionic stress also significantly impacts CO_2 availability by causing the closure of stomata, which restricts the diffusion of CO_2 into the chloroplasts. This results in a decrease in intracellular CO_2 concentration, limiting the activity of Calvin-Benson cycle enzymes, particularly ribulose-1,5-biphosphate carboxylase/oxygenase (RuBisCo) (Tokarz et al., 2021).

Osmotic stress, along with water stress and ion toxicity, can also manifest as oxidative stress. As previously discussed, when plants are subjected to these abiotic stresses, they respond by closing stomata, which reduces the CO_2/O_2 ratio in the leaves and inhibits CO_2 fixation. This results in an increased electron leak to oxygen, leading to a higher rate of formation of reactive oxygen species (ROS), such as superoxide (O_2^-), hydrogen peroxide (H_2O_2), hydroxyl radicals (·HO), and singlet oxygen ($^1O_2$) (Hernández & Almansa, 2002).

Furthermore, water stress also leads to the photoinhibition process, because there is a decrease in photosynthetic efficiency without a reduction of the intensity of photosynthetically active radiation (PAR). This causes an excess of untapped energy that damages the photosynthetic apparatus and consequently generates more ROS (Tokarz et al., 2021). As a result, the equilibrium between the generation of ROS and the efficacy of antioxidant mechanisms is perturbed, leading to increased oxidative damage (Hernández et al., 1999).

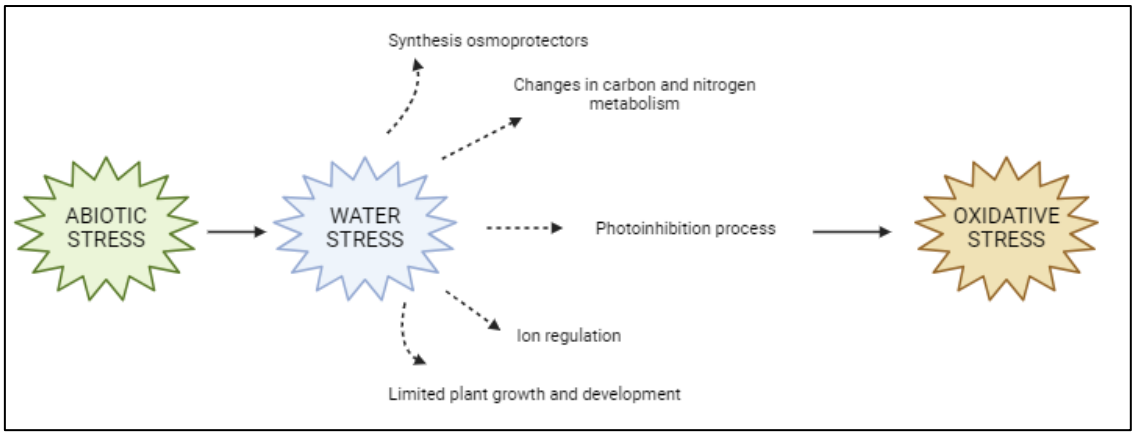

Figure 1. Overview of how water stress affects plants and can lead to oxidative stress. *Adapted from Tokarz et al. (2021).*

When the plant's defense mechanisms against oxidative damage are overwhelmed by increased ROS production, oxidative stress occurs. At this stage, there is an accumulation of ROS that targets DNA, lipids, proteins, and carbohydrates. This results in abnormal metabolic function in plants and can lead to lipid peroxidation (LP), protein denaturation, and DNA mutations (Mangal et al., 2023).

Polyunsaturated fatty acids (PUFAs) are lipid components that are commonly and readily oxidized by ROS. When ROS reacts with PUFAs, a sequence of lipid peroxidation reactions is initiated. It begins with the separation of an allylic hydrogen atom from the PUFAs, resulting in the formation of a lipid radical. This radical reacts with molecular oxygen to form lipid peroxyl and lipid alkoxyl radicals, both of which cause a chain reaction of radical oxidation as they react with neighboring lipid molecules (Alché, 2019).

This leads to changes in membrane structure and its physical properties, such as permeability to different compounds, and can ultimately result in the loss of normal cell and tissue function, followed by cell death (Mangal et al., 2023).

A product of lipid peroxidation is malondialdehyde (MDA), which forms as a result of lipid oxidation and breakdown. MDA is used as a marker to assess cell membrane integrity and the level of oxidative damage, as plants produce more MDA under stress conditions (Ashraf et al., 2023).

In order to prevent the excessive accumulation of ROS during stress and to mitigate or repair the damage initiated by ROS, plants develop protective mechanisms in the form of antioxidant compounds and enzymes. Primary elements of this system include, among others, glutathione, and enzymes involved in the ascorbate-glutathione cycle such as glutathione reductase (GR) (Tokarz et al., 2021).

Reduced glutathione (GSH) is the most abundant low molecular weight thiol compound in plants. It has unique structural properties and a wide redox spectrum. Its stability derives from the γ-glutamyl bond, while the strong nucleophilic nature of its central Cys confers strong reducing properties. Actually, it is the major cellular antioxidant present in plants, providing protection against a wide range of peroxides, xenobiotics, and heavy metals.

GSH is synthesized from its constituent amino acids through a two-step ATP-dependent reaction, catalyzed by the enzymes γ-glutamylcysteine synthetase (γ-ECS) and glutathione synthetase (GSH-S). These enzymes have been partially characterized and have been found to be present in both chloroplasts and cytosolic compartments.

Furthermore, GSH synthesis has been shown to be regulated by three mechanisms: the amount of γ-ECS activity, substrate availability, and, to a smaller extent, feedback inhibition by γ-ECS and GSH. Moreover, γ-ECS activity is transcriptionally and translationally regulated by the GSH:GSSG ratio (Mittova et al., 2003).

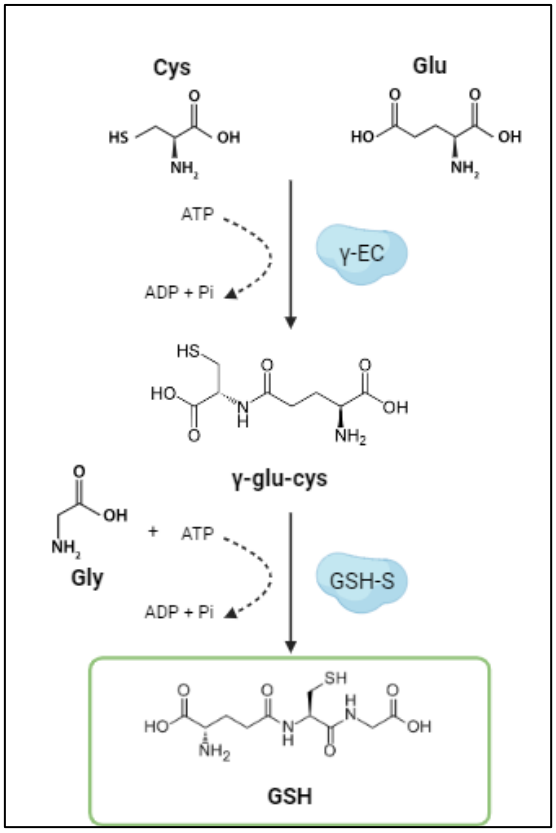

Figure 2. GSH synthesis pathway. *Cys, cysteine; Glu, glutamic acid; Gly, glycine; γ-ECS, glutamylcysteine synthase; GSH-S, glutathione synthetase; GSH, reduced glutathione. Adapted from Mittova et al. (2003).*

In addition to its antioxidant functions, nitric oxide (NO) in the presence of oxygen can react with GSH to form S-nitrosoglutathione (GSNO), a reactive nitrogen species (RNS). This compound can be formed within peroxisomes and can act as a signaling molecule, transporting NO-bound GSH to organelles or neighboring cells and throughout the plant (Romero-Puertas et al., 2006).

As previously mentioned, GSH is the primary antioxidant present in plants. The thiol group of this compound can be oxidized to form GSSG, which is incapable of protecting against oxidation. Therefore, maintaining high cellular ratios of GSH:GSSG is essential for preserving the redox state of the cell (Mittova et al., 2003).

In plants, glutathione reductase (GR) is the enzyme responsible for converting GSSG to its reduced form (GSH), with the simultaneous oxidation of NADPH. This reaction is part of the ascorbate-glutathione cycle, which removes hydrogen peroxide (H_2O_2) with the coordination of

three other enzymes: ascorbate peroxidase (APX), monodehydroascorbate reductase (MDAR), and dehydroascorbate reductase (DAR).

GR has been primarily located in chloroplasts, mitochondria, the cytosol, and also in peroxisomes. Within these organelles, two enzymes of the ascorbate-glutathione cycle were found to be inserted in the peroxisomal membrane (APX and MDAR), while GR and DAR were located in the peroxisomal matrix.

The distribution of this enzymatic system across different organelles suggests that distinct topogenic signals target different cellular compartments. This is relevant from the perspective of differential regulation of various isoenzymes under stress conditions in plants (Romero-Puertas et al., 2006).

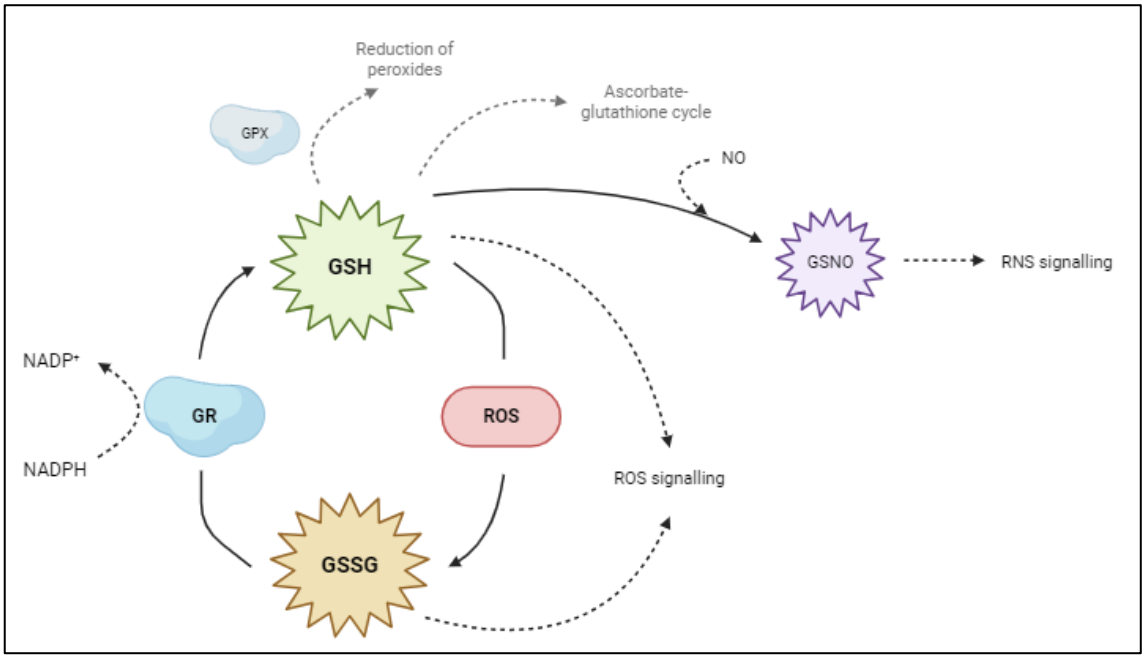

Figure 3. General overview fo some of the most important glutathione functions *(redox turnover, metabolism, signalling). GSH, reduced glutathione; GSSG, oxidized glutathione; GSNO, S-nitrosoglutathione; GPX, glutathione peroxidase; GR, glutathione reductase; NO, nitric oxide; ROS, reactive oxygen species; RNS, reactive nitrogen species. Adapted from Noctor et al. (2012).*

Peas are a leguminous crop cultivated in cold climates and hold the distinction of being the third most significant legume in the human diet. They are esteemed for their elevated protein content (25-35%) and essential amino acids. Additionally, peas serve as a notable reservoir of carbohydrates, minerals such as calcium and iron, and vitamins including thiamine, tocopherol, niacin, and folic acid (Lu et al., 2020).

In particular, the species *Pisum sativum L.* exhibits a relatively high demand for water during its growth period, notably during germination and flowering, making it highly vulnerable to water deficiency and osmotic stress. Generally, induction of abiotic stress in peas is associated with deleterious impacts on growth dynamics, biomass production, flower abortion, and seed yield reduction. Furthermore, metabolism in the roots and nodules can be affected, leading to abnormal distribution of assimilated carbon and nitrogen throughout the plant, along with an increase in ROS formation and subsequent onset of oxidative stress (Szablińska-Piernik & Lahuta, 2021).

Polyethylene glycol (PEG) is a neutral water-soluble polymer that has been commonly employed as an osmotic agent in various contexts, including the whole plant, tissues, cells, and organelles. They are utilized to investigate the effects of water deficit on plants by increasing osmotic pressure, thereby reducing the available water for plant uptake (Popović et al., 2017).

This work is part of a large-scale multidisciplinary project called TowArds Next GENeration Crops (TANGENC), which is funded by a grant from the European Union and administered by the Ministry of Education of the Czech Republic.

This multidisciplinary project focuses on plant responses to unfavorable environmental conditions, and its purpose is to present novel insights and discoveries about molecular mechanisms involved in the growth and development of plants in response to these environmental stimuli. The fundamental aims of this research project are:

(i) To uncover the mechanisms involved in responding to abiotic stress during critical phases of plant growth and development.
(ii) To optimize biotechnological procedures for utilizing new findings in breeding.
(iii) To support the transfer of new knowledge into breeding practice.
(iv) To raise public awareness of new breeding techniques.

Specifically, this research is part of activity (i).2 of this project. It focuses on identifying key components of the redox regulatory system in plant seeds and the early stages of life, by quantifying and visualizing reactive oxygen species (ROS) and reactive nitrogen species (RNS), while also analyzing the enzymatic activities of the ROS scavenging system. The principal goal is to identify the key elements of the regulatory pathways that became activated during early growth in response to water limitation.

As mentioned, one of the greatest challenges currently facing us is ensuring an adequate food supply for the growing population under changing climatic conditions, and doing so sustainably. Therefore, there is a critical need to expand our current understanding of the molecular mechanisms underlying crop defense against various types of abiotic stresses, including water deficit stress, and to intensify research efforts to better comprehend crop responses to these adversities. In the long term, this will provide targets for molecular genetic improvement to develop crops resistant to drought, soil salinity, or high temperatures.

3. HYPHOTESIS AND OBJECTIVES

In summary, in response to water deficit, plants develop osmotic adjustment as a primary defense mechanism, although it often results in oxidative stress. To counteract the excessive accumulation of ROS during stress, plants employ protective mechanisms in the form of antioxidant compounds and enzymes to mitigate the detrimental effects of oxidative stress and ensure plant resilience under adverse environmental conditions. Key components of this system include glutathione and enzymes such as glutathione reductase (GR). And, therefore, in unfavorable conditions for plant growth and development, both the biosynthesis of antioxidant compounds and the activity of antioxidant enzymes change.

Key hypotheses have already been formulated, focusing on whether water stress would induce oxidative damage in *Pisum sativum L.*, and consequently, an increase in lipid peroxidation. Additionally, it was hypothesized that stress would reduce the GSH:GSSG ratio, while increasing GR activity. Finally, it was proposed that there would be a correlation between oxidative stress and an increase in SNO.

Accordingly, the main objective of this work is to understand the effect of water deficit and osmotic stress on the early stages of pea (*Pisum sativum L.*) growth. Specifically, to understand how it affects the antioxidant mechanisms related to glutathione.

4. MATERIALS AND METHODS

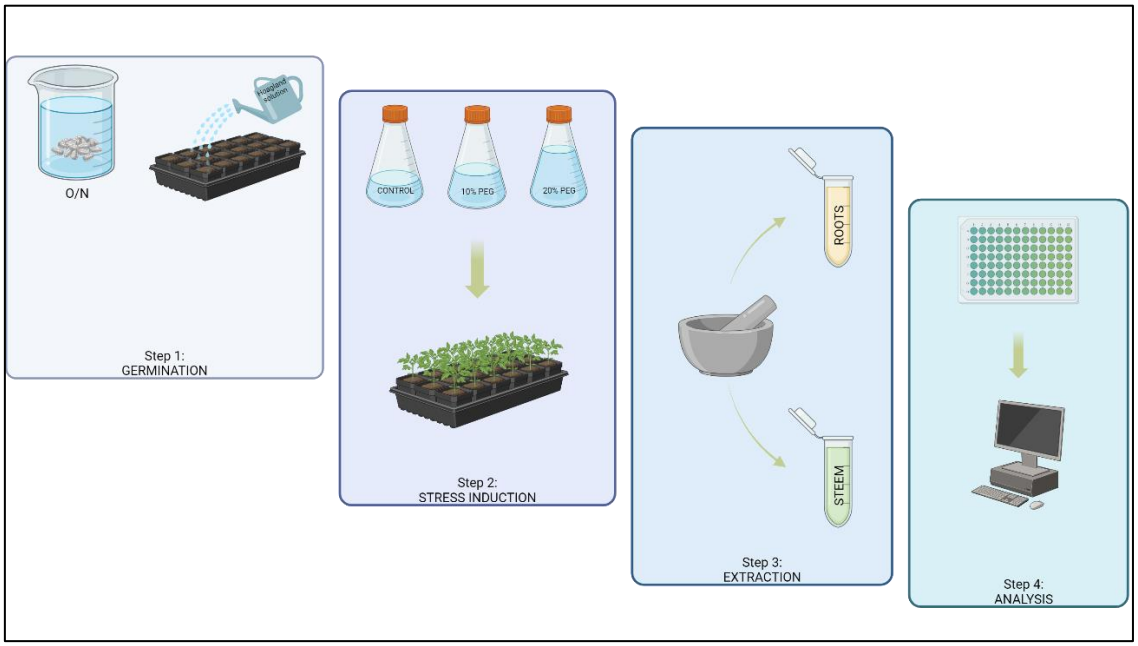

Figure 4. Overview of experimental procedures.

To achieve the above mentioned objectives, the following steps were undertaken:

(i) To induce water stress in peas at the beginning of germination using PEG.
(ii) To quantify the concentrations of GSH and GSSG in roots and shoots.
(iii) To determine the change in the activity of the enzyme GR in roots and shoots.
(iv) To quantify the concentration of SNO in roots and shoots.

4.1. Plant material. Pea seeds (*Pisum sativum L.*) commercially available were soaked in tap water overnight and then planted in 6 containers filled with Perlit EP AGRO layer (Perlit, Šenov u Nového Jičína, Czech Republic) and allowed to germinate. Over the course of two weeks, the seedlings were regularly irrigated with Hoagland solution, comprising the following composition: KNO_3 (1500µM), $Ca(NO_3)_2{\cdot}H_2O$ (1000µM), $NH_4H_2PO_4$ (500µM), $MgSO_4{\cdot}7H_2O$ (250µM), KCl (50µM), $MnSO_4{\cdot}H_2O$ (2µM), $ZnSO_4{\cdot}7H_2O$ (2µM), $CuSO_4{\cdot}5H_2O$ (0.5µM), $(NH_4)_6Mo_7O_{24}{\cdot}4H_2O$ (0.5µM), H_3BO_3 (12.5µM) and FeEDTA (20µM). Plants were grown in a growth chamber with controlled temperature (21ºC during day and 18ºC at night), 15h daylight, and a light intensity of 100 µE/m/s.

4.2. Stress induction. Various water stress conditions were induced using PEG diluted with Hoagland solution: (A) 0% PEG solution (experimental control), (B) 10% PEG solution, and (C) 20% PEG solution. Each condition was duplicated. Subsequently, 100ml of each solution was applied every two days over a period of one week to the soil of the growing plants.

4.3. Preparation of plant tissue homogenates. Roots and shoots were separated. Two distinct extraction protocols were carried out using different buffers depending on the

compounds to be determined. For lipid peroxidation evaluation, 0.5g of each component was weighed and ground using a mortar and pestle. Subsequently, 5ml of a buffer solution comprising 0.1% trichloroacetic acid and 0.00005% butyl-hydroxytoluene was added. For other determinations, 2g of each plant part was weighed and ground, with the addition of 4x volume of 100mM phosphate buffer (pH=7,5). This extraction buffer contained 40mM KH_2PO_4, 60mM K_2HPO_4, 2mM EDTA-Na^+, 1% PVPP, 2mM DTT, and 0.5mM pefabloc. In both procedures, the homogenate underwent centrifugation at 16000x g for a duration of 10 minutes, and the supernatant was collected and frozen for further analysis. The remaining plant samples were frozen at -30ºC for subsequent use.

4.4. Protein assay. The determination of total protein content was conducted employing the Bradford method(Zor & Selinger, 1996). A stock solution of Coomassie Blue, comprising 50mg Coomassie Blue G250 dissolved in 25ml ethanol and 50ml 85% phosphoric acid, was diluted with distilled water (ddH_2O) in a 1:4 ratio. Furthermore, a series of standards of bovine serum albumin (BSA) were prepared through successive dilutions of 1, 5, 10, 25, 50, 75, 100, 250, 500, 750 and 1000 µg/ml, derived from a BSA stock solution (2mg/ml). In a microplate, ddH_2O, the working solution of Bradford's reagent, along with the samples or standards were added. A blank was established using ddH_2O, and triplicates were generated for each experimental condition. Finally, the absorbance ratio at 590/450nm was evaluated against the protein concentration.

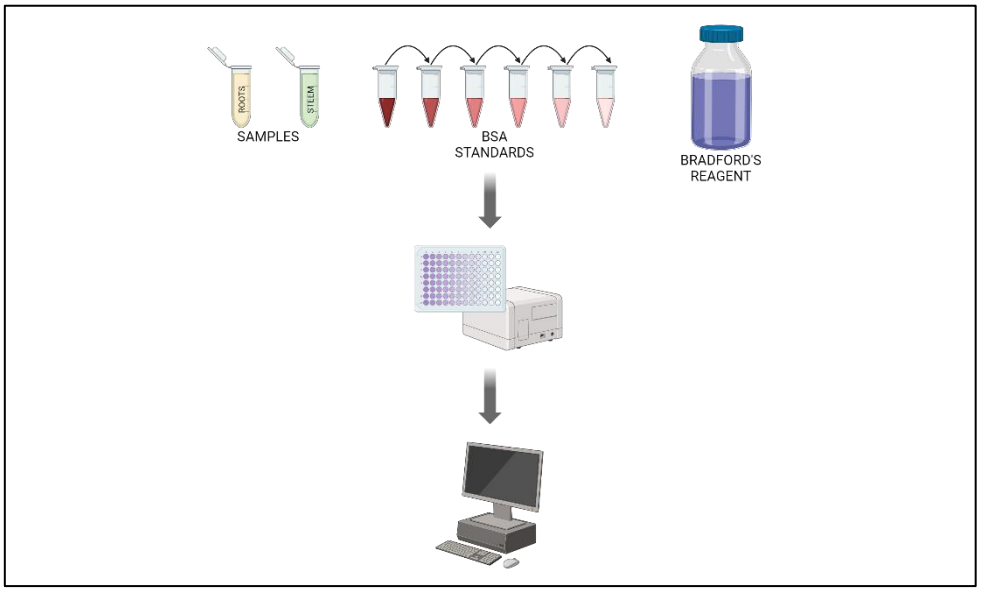

Figure 5. Protein assay framework*. Adapted from* (Zor & Selinger, 1996).

4.5. Determination of lipid peroxidation. The malondialdehyde (MDA) or thiobarbituric acid-reactive substances (TBARS) assay was conducted to estimate lipid peroxidation (Hodges et al., 1999). MDA is a secondary product of oxidation and enzymatic degradation of polyunsaturated fatty acids present in cells. This compound reacts with two molecules of thiobarbituric acid (TBA) via a nucleophilic addition catalyzed by an acid, resulting in the formation of a pink-red chromogen with a maximum absorbance at 532nm. Two distinct reagents were utilized in this assay: reagent A, comprising 20% trichloroacetic acid and 0.01% butyl-hydroxytoluene, which served as a control, and reagent B, supplemented with 0.65% TBA, which facilitated the reaction with MDA. A standard curve was constructed using MDA as standard with serial dilution

concentrations of 0.1, 0.5, 1, 2.5, 5, 7.5 and 10µM. Each sample was measured with both reagent A and reagent B. In an Eppendorf tube, 0.5ml of sample or standard and 0.5ml of reagent A or reagent B were added. The mixture was subjected to thermal treatment at 90ºC for 25 minutes in a thermoblock and subsequently cooled in an ice bath. Following centrifugation at 1500 x g for 10 minutes, the supernatant was transferred to a microplate, and absorbance readings at 440, 532 and 600nm were recorded. As mentioned, the content of MDA can be determined by measuring absorbance at 532nm, but there are different compounds that can interfere, and it is necessary to eliminate their potential contribution. Therefore, it is also necessary to measure absorbance at 440nm and 600nm. Triplicates of each sample were performed.

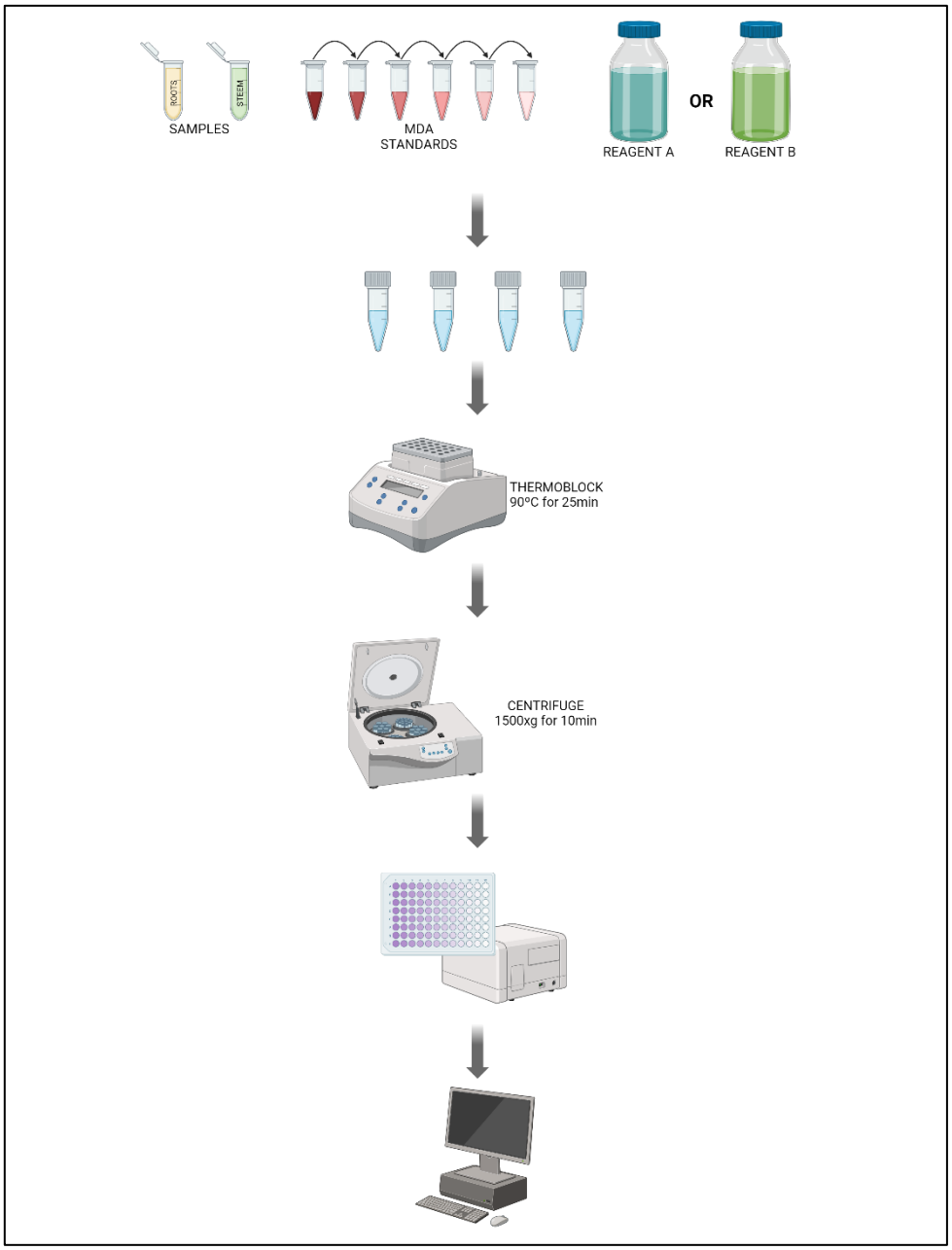

Figure 6. Lipid peroxidation determination framework. *Adapted from (Hodges et al., 1999).*

4.6. Determination of the content of S-nitrosothiols, GSH and GSSG. The Saville method was employed for the determination of S-nitrosothiols. This is a colorimetric method, as S-

nitrosothiols release the nitrosonium ion (NO^+) through a reaction catalyzed by mercury salts (Hg^{2+}), resulting in the formation of nitrite. Nitrite is subsequently detected through the formation of a diazonium salt in an acidic medium and its copulation with N-(1-naphthylethylene)diamine (NED) to yield an azo dye (Gow et al., 2007). For this method, three different reagents are needed: reagent A composed of 3.5% sulfanilamide in 0.5M HCl, reagent B to which 1% $HgCl_2$ is added, and NED reagent containing 0.1% NED in ddH_2O. Furthermore, two calibration curves were also established using sodium nitrite ($NaNO_2$) in ddH_2O and S-nitrosoglutathione (GSNO) in 0.5M HCl as standards. Serial dilutions were made with concentrations of 5, 10, 25, 50, 100, 250 and 500µM. Samples or standards and reagents were added to a microplate, considering that reagent A was employed for the $NaNO_2$ standard and the blank was made with ddH_2O, and reagent B was used for the GSNO standard and the blank was made with 0.5M HCl. The mixture was incubated at room temperature for 5 minutes, and then NED reagent was added in order to start the reaction. Finally, it was incubated for an additional 5 minutes, also at room temperature, and the absorbance at 540nm was measured. Triplicates of each sample were performed again.

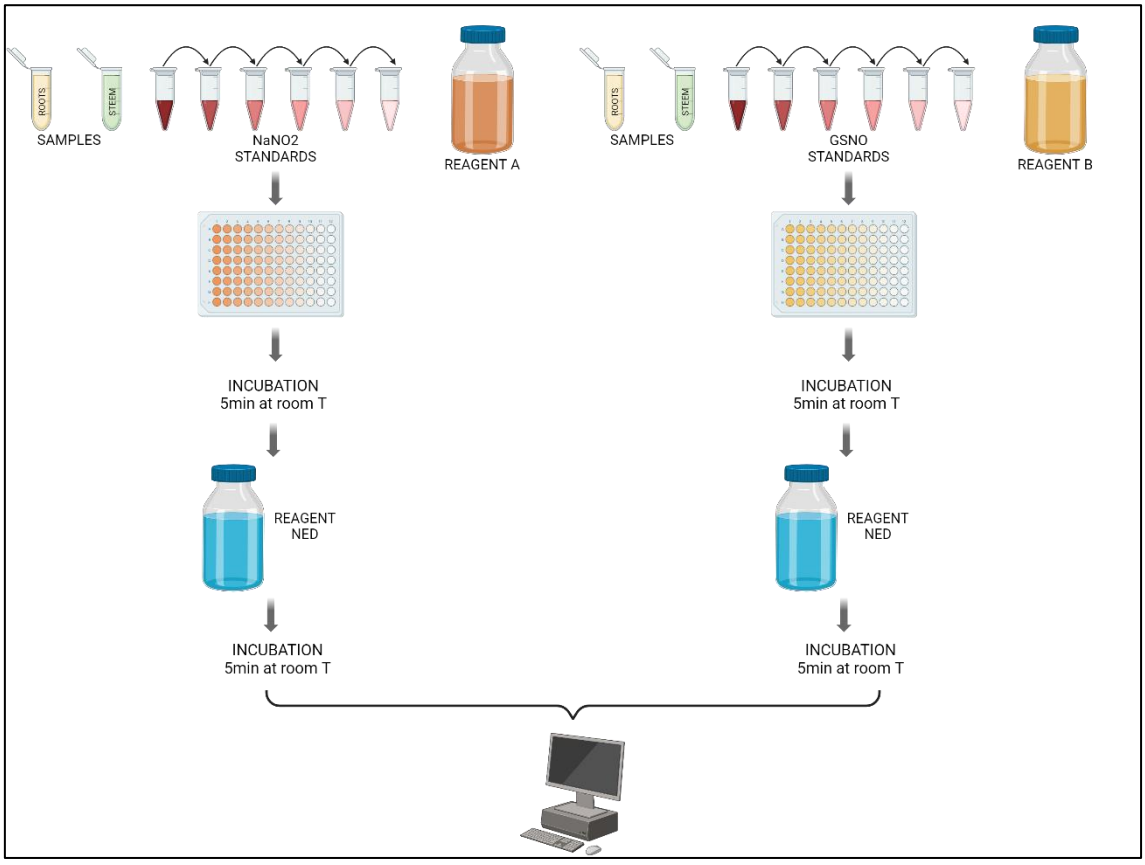

Figure 7. S-nitrosothiols determination framework. *Adapted from (Gow et al., 2007).*

For the quantification of glutathione content, both reduced (GSH) and oxidized (GSSG), a fluorescent method with monobromobimane (MBB) was employed. In this assay, GSH reacts with MBB to generate a fluorescent adduct, readily detectable through fluorescence. Conversely, GSSG levels were determined by first measuring both total glutathione levels and GSH levels, followed by subtraction of GSH levels from the total (Anderson et al., 1999). A 100mM TRIS/HCl buffer solution (pH=8.0), a 15mM MCIB solution in acetonitrile, and a 5mM TCEP solution in

buffer were required. Furthermore, calibration curves were established using GSH and GSSG at concentrations of 1, 5, 10, 50, 100, 250 and 500µM in buffer. Samples or standards and the buffer were added to a microplate. To measure total glutathione levels, 20µl of a 5mM TCEP solution were added, whereas for the specific quantification of GSH, 20µl of buffer were utilized instead. The mixture was then incubated for 20 minutes, and the reaction was initiated with the 15mM MCIB solution. After another 20 minute incubation, this time in darkness, the increase in fluorescence was measured (excitation 360nm/emission 460nm). Blank measurements were conducted using buffer, and triplicates of each sample were analyzed.

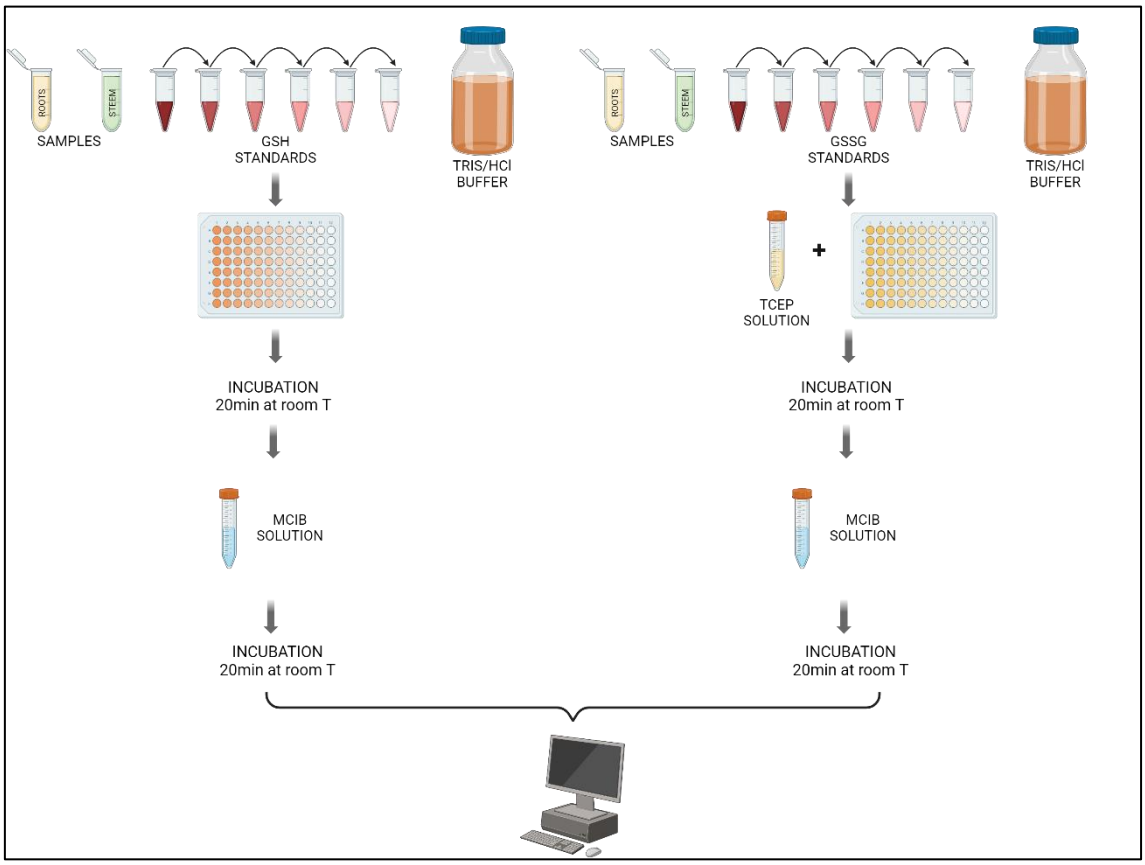

Figure 8. Glutathione determination framework*. Adapted from (Anderson et al., 1999).*

4.7. Measurement of enzyme activity. The determination of glutathione reductase (GR, EC 1.6.4.2) enzyme activity was conducted utilizing a spectrophotometry method (Mannervik, 1999). The activity was measured by the decrease in absorbance caused by the oxidation of NADPH at 340nm, absorbance readings were recorded at 30-second intervals over a period of 6 minutes. In a microplate, the reaction mixture composed of 2mM NADPH, 20mM GSSG, and 100mM phosphate buffer (pH=7.5) containing 40mM KH_2PO_4, 60mM K_2HPO_4 and 2mM EDTA-Na^+ was added. Subsequently, the mixture was incubated at 30ºC for 3 minutes, following which the enzymatic reaction was initiated by the addition of the sample. The blank was prepared using the 100mM phosphate buffer.

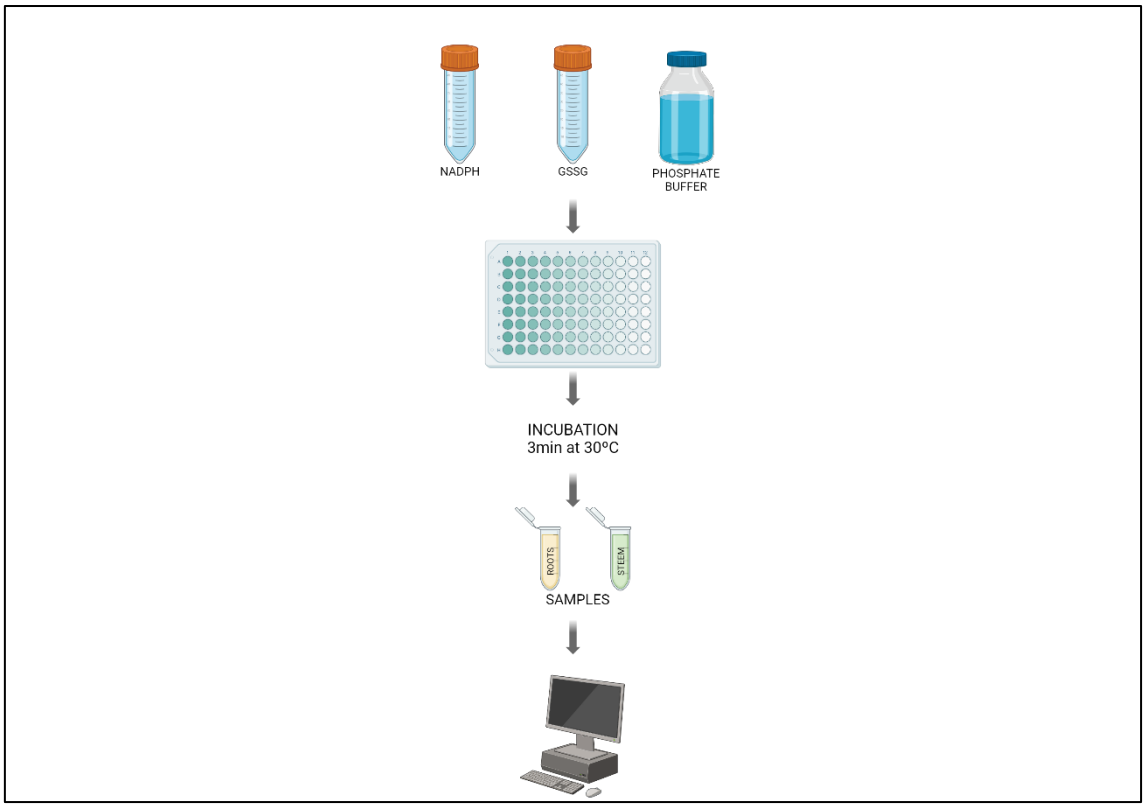

Figure 9. Glutathione reductase activity determination framework. *Adapted from (Mannervik, 1999).*

5. RESULTS

5.1. The administration of PEG increases the total protein concentration in Pisum sativum L.

The total protein concentration in the samples (*Table 1*) was determined utilizing the standard curve derived from dilutions of BSA standards: $y = 0.0012x + 1.1497$ (R^2=0.9931). Due to deviation from the standard curve, a 1/10 dilution was applied to the root samples. This adjustment was taken into consideration in the calculation of the final sample concentrations.

Table 1. Total protein content using the Bradford assay. *The concentrations have been calculated following the standard curve* $y = 0.0012x + 1.1497$ *with* R^2*=0.9931.*

TREATMENT		RATIO 590/450NM			MEAN ± SD	[ ] (µG/ML)
CONTROL	Stem	1,314	1,223	1,307	1,2813±0,05	1096,9444±421,99
	Roots	1,283	1,264	1,301	1,2827±0,02	110,8056±15,42
10% PEG	Stem	1,462	1,335	1,405	1,4007±0,06	2091,3889±530,09
	Roots	1,51	1,497	1,482	1,4963±0,01	288,8611±11,68
20% PEG	Stem	1,43	1,458	1,386	1,4247±0,03	2291,3889±302,46
	Roots	1,437	1,426	1,439	1,434±0,007	236,9167±5,83

As observed in *Table 1*, the protein concentration increased due to water stress induced by PEG administration. Across all three conditions, the values obtained in the stem are higher compared to those in the roots. Although the protein content is higher in the samples treated with PEG compared to the control, the magnitude of augmentation varies in different parts of the plant depending on the applied concentration. In the case of the stem, the protein content is higher after treatment with a concentration of 10%, whereas in the roots, the content is higher with the 20% PEG treatment. *Figure 10* illustrates a comparative analysis among the three conditions: control (C), 10% PEG solution (10%), and 20% PEG solution (20%), as well as the differences between the stem (S) and the roots (R).

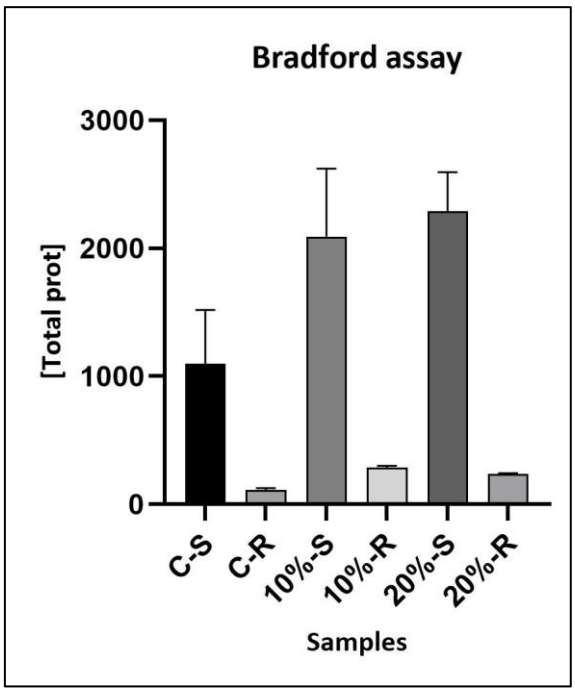

Figure 10. **Bar chart illustrating the levels of total proteins in the different samples.** The protein concentration is expressed in µg/ml. From left to right, the samples are as follows: stem control (C-S), root control (C-R), stem treated with 10% PEG solution (10%-S), roots treated with 10% PEG solution (10%-R), stem treated with 20% PEG solution (20%-S), and roots treated with 20% PEG solution (20%-R). P value < 0,0001.

5.2. Lipid peroxidation increases with PEG administration in both stems and roots.

In *Table 2*, one can observe the different absorbance obtained in the control samples, or treated with reagent A. Likewise, the absorbance values obtained from samples treated with reagent B are presented in *Table 3*.

Table 2. Absorbance values at 440, 532 and 600nm of the samples treated with reagent A.

	TREATMENT					
	CONTROL		**10% PEG**		**20% PEG**	
	Stem	Roots	Stem	Roots	Stem	Roots
ABS 440	0,076	0,091	0,085	0,076	0,133	0,501
	0,077	0,078	0,074	0,077	0,151	0,413
	0,082	0,113	0,084	0,077	0,172	0,581
MEAN±SD	0,0783±0,003	0,094±0,02	0,081±0,006	0,0767±0,001	0,152±0,02	0,4983±0,08
ABS 532	0,063	0,073	0,068	0,058	0,104	0,39
	0,064	0,063	0,058	0,063	0,128	0,329
	0,07	0,085	0,063	0,061	0,131	0,49
MEAN±SD	0,0657±0,003	0,0737±0,01	0,063±0,005	0,0607±0,003	0,121±0,01	0,403±0,08
ABS 600	0,058	0,066	0,064	0,055	0,091	0,361
	0,06	0,058	0,056	0,057	0,121	0,283
	0,065	0,071	0,06	0,057	0,115	0,432
MEAN±SD	0,061±0,003	0,065±0,004	0,06±0,004	0,0563±0,001	0,109±0,02	0,3587±0,07

Table 3. **Absorbance values at 440, 532 and 600nm of the samples treated with reagent B**.

	TREATMENT					
	CONTROL		**10% PEG**		**20% PEG**	
	Stem	Roots	Stem	Roots	Stem	Roots
ABS 440	0,167	0,124	0,164	0,102	0,421	0,118
	0,156	0,124	0,162	0,116	0,411	0,105
	0,169	0,091	0,161	0,108	0,425	0,178
MEAN±SD	0,164±0,007	0,113±0,02	0,1623±0,001	0,1087±0,01	0,419±0,01	0,1337±0,04
ABS 532	0,241	0,135	0,269	0,122	0,341	0,14
	0,225	0,132	0,263	0,131	0,337	0,125
	0,238	0,107	0,261	0,137	0,345	0,185
MEAN±SD	0,2347±0,01	0,1247±0,02	0,2643±0,004	0,13±0,01	0,341±0,004	0,15±0,03
ABS 600	0,058	0,074	0,054	0,058	0,074	0,067
	0,057	0,076	0,054	0,062	0,074	0,062
	0,063	0,052	0,05	0,079	0,079	0,113
MEAN±SD	0,0593±0,003	0,0673±0,01	0,0527±0,002	0,0663±0,011	0,0757±0,003	0,0807±0,03

In order to determine the concentration of MDA present in each sample, an evaluation of the data was necessary. The following formula, described inHodges et al. (1999), was utilized to obtain the MDA equivalents.

$$A = (Abs_{532+TBA}) - (Abs_{600+TBA}) - (Abs_{532-TBA} - Abs_{600-TBA})$$

$$B = (Abs_{440+TBA} - Abs_{600+TBA}) \times 0{,}0571$$

$$MDA\ equivalents\ \left(\frac{nmol}{ml}\right) = \frac{A - B}{157000} \times 10^6$$

Initially, the MDA equivalents of the standards were calculated and represented on a calibration curve alongside known MDA concentrations. The resulting equation of the calibration curve was $y = 0.58873x + 0.1989$ (R^2=0,998). Subsequently, the MDA equivalents of the control samples and those treated with 10% PEG and 20% PEG solutions were calculated. Employing the established calibration curve, the concentration of MDA present in each sample was determined. The obtained results are presented in *Table 4*.

Table 4. **MDA content following the TBARS method**. The final concentrations have been calculated using the standard curve equation $y = 0.58873x + 0.1989$ with R^2=0,998.

TREATMENT		A	B	MDA EQUIVALENTS (NMOL/ML)	[ ] (µMOL/ML)
CONTROL	Stem	0,3507±0,015	0,0070±0,0003	2,1892±0,09	3,3889±0,16
	Roots	0,1147±0,006	0,0043±0,0004	0,7032±0,04	0,8587±0,07
10% PEG	Stem	0,4233±0,006	0,0075±0,0003	2,6489±0,04	4,1716±0,07
	Roots	0,1273±0,011	0,0036±0,0007	0,7882±0,07	1,0035±0,11
20% PEG	Stem	0,5307±0,004	0,0221±0,001	3,2395±0,02	5,1773±0,04
	Roots	0,1387±0,011	0,0110±0,0012	0,8132±0,06	1,0459±0,11

Analyzing *Table 4* and the graphical representation in *Figure 11*, it is evident that under all conditions, the concentration of MDA is higher in the stem compared to the roots. Additionally, it can be observed that water stress induced by the administration of different PEG solutions leads to an increase in lipid peroxidation, as evidenced by the elevated MDA content. However, comparing the concentrations obtained in the roots and stems after administering 10% PEG and 20% PEG solutions, it is notable that the difference in the stem is relatively higher compared to the difference in concentrations in the roots.

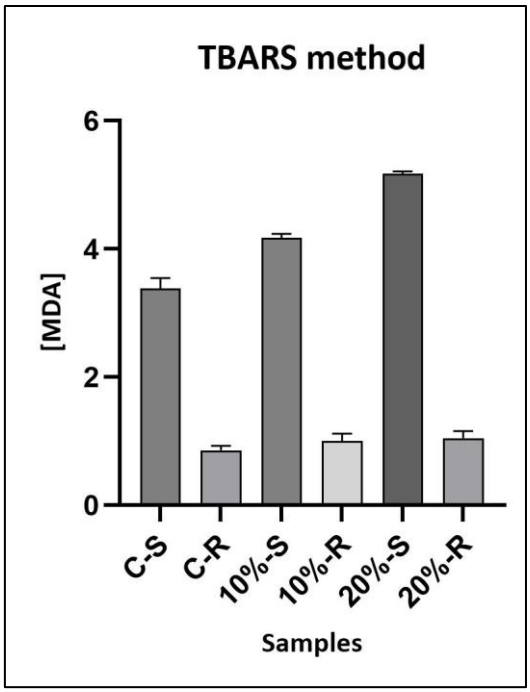

Figure 11. **Bar chart describing the levels of MDA in the different samples**. MDA concentrations are expressed in µmol/ml. From left to right, the samples are as follows: stem control (C-S), root control (C-R), stem treated with 10% PEG solution (10%-S), roots treated with 10% PEG solution (10%-R), stem treated with 20% PEG solution (20%-S), and roots treated with 20% PEG solution (20%-R). P value < 0,0001.

5.3. Administration of 20% PEG increases the concentration of S-nitrosothiols in the stem.

The absorbance obtained from the different samples treated with reagent A (3.5% sulfanilamide in 0.5M HCl), and reagent B (3.5% sulfanilamide in 0.5M HCl + 1% $HgCl_2$), can be observed in *Table 7*.

Table 7. **Absorbance values at 540nm of the different samples.** The values obtained in the samples treated with reagent A (3.5% sulfanilamide in 0.5M HCl) correspond to free nitrites, while the values obtained with reagent B (3.5% sulfanilamide in 0.5M HCl + 1% $HgCl_2$) correspond to total nitrites.

		TREATMENT					
		CONTROL		**10% PEG**		**20% PEG**	
		Stem	Roots	Stem	Roots	Stem	Roots
ABS 540NM	**Reagent A**	0,068	0,052	0,059	0,05	0,085	0,052
		0,064	0,057	0,061	0,054	0,093	0,049
		0,061	0,05	0,074	0,052	0,072	0,053
	Mean ± SD	0,0643±0,004	0,053±0,004	0,0647±0,008	0,052±0,002	0,0833±0,01	0,0513±0,002
	Reagent B	0,135	0,052	0,107	0,062	0,141	0,057
		0,117	0,06	0,093	0,067	0,129	0,058
		0,124	0,058	0,093	0,068	0,157	0,062
	Mean ± SD	0,1253±0,009	0,0567±0,004	0,0977±0,008	0,0657±0,003	0,1423±0,01	0,059±0,002

The concentration of free nitrites and total nitrites were determined by employing two distinct calibration curves. In the first case, calibration was executed utilizing $NaNO_2$ standards and reagent A, yielding the following regression equation: $y = 0{,}0014x + 0{,}0452$ (R^2=0,9999). For the quantification of total nitrites, reagent B was employed, and a separate calibration curve was established utilizing GSNO standards, resulting in the equation: $y = 0{,}0005x + 0{,}0484$ (R^2=0,9992). Subsequently, the final concentration of SNO was calculated using the following formula as described in Gow et al. (2007):

$$SNO = (total\ nitrites) - (free\ nitrites)$$

Table 8. SNO content determined via the Saville Method. *Free nitrite concentrations were determined utilizing the standard curve* $y = 0{,}0014x + 0{,}0452$ *with* R^2=0,9999*, while total nitrite concentrations were calculated using the curve* $y = 0{,}0005x + 0{,}0484$ *with* R^2=0,9992*. The final SNO concentration corresponds to the difference between the two previously mentioned concentration values.*

TREATMENT		[FREE NITRITES] (µMOL/L)	[TOTAL NITRITES] (µMOL/L)	[SNO] (µMOL/L)
CONTROL	Stem	13,6667±2,51	153,8667±18,15	140,2±16,57
	Roots	5,5714±2,58	16,5333±8,33	10,9619±7,48
10% PEG	Stem	13,9048±5,82	98,5333±16,17	84,6286±20,21
	Roots	4,8571±1,43	34,5333±6,43	29,6762±5,39
20% PEG	Stem	27,2381±7,57	187,8667±28,09	160,6286±35,66
	Roots	4,3809±1,49	21,2±5,29	16,8190±4,65

As observed in both *Table 8* and *Figure 12*, the SNO concentration is higher in the stem compared to the roots. However, in this case, the water stress induced by PEG administration does not uniformly increase SNO content under all conditions. This is exemplified by the higher SNO concentration in the control stem sample compared to the stem sample treated with a 10% PEG solution. Nevertheless, under other conditions, water stress does lead to an increase in SNO concentrations. It is also noteworthy how stress affects different parts of the plants differently; while the highest SNO content in roots is observed with the administration of a 10% PEG solution, the stem manifests a higher SNO concentration with a 20% PEG solution.

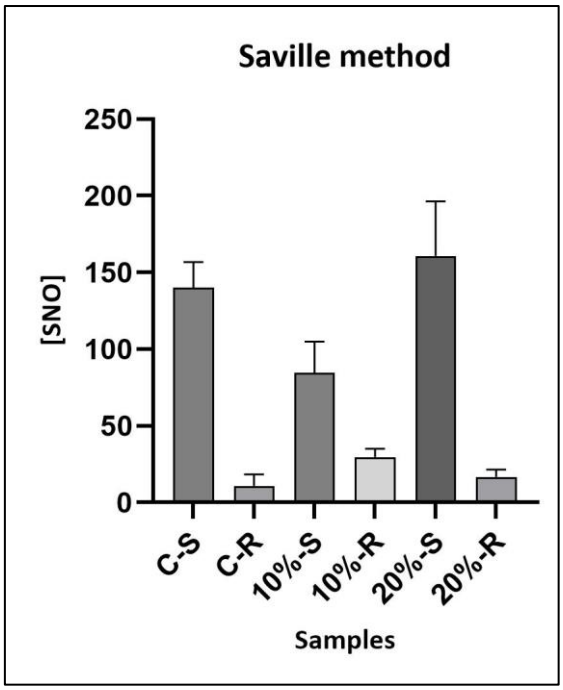

Figure 12. **Bar graph illustrating the SNO levels of various samples.** SNO concentrations are measured in µmol/l. From left to right, the samples are as follows: stem control (C-S), root control (C-R), stem treated with 10% PEG solution (10%-S), roots treated with 10% PEG solution (10%-R), stem treated with 20% PEG solution (20%-S), and roots treated with 20% PEG solution (20%-R). P value < 0,0001.

5.4. Glutathione reductase activity increases with PEG administration.

To determine changes in the activity of the enzyme GR, absorbance was measured at 30-second intervals over a duration of 6 minutes. The resulting values are presented in *Table 9*.

Table 9. Absorbance values at 340nm of the samples. *The average of triplicates has been calculated along with the standard deviation.*

	TIME (MIN)	TREATMENT					
		CONTROL		10% PEG		20% PEG	
		Stem	Roots	Stem	Roots	Stem	Roots
ABS 340NM	0,5	0,5013±0,008	0,4250±0,012	0,5330±0,031	0,4557±0,017	0,5893±0,013	0,4683±0,008
	1	0,4800±0,009	0,4190±0,013	0,5150±0,028	0,4600±0,01	0,5593±0,009	0,4663±0,008
	1,5	0,4767±0,01	0,4193±±0,011	0,5043±0,03	0,4583±0,012	0,5400±0,016	0,4620±0,009
	2	0,4710±0,009	0,4223±0,013	0,4890±0,027	0,4563±0,013	0,5207±0,019	0,4587±0,006
	2,5	0,4637±0,006	0,4247±0,013	0,4727±0,024	0,4557±0,014	0,4983±0,014	0,4560±0,004
	3	0,4557±0,005	0,4253±0,013	0,4573±0,023	0,4543±0,013	0,4783±0,013	0,4523±0,006
	3,5	0,4470±0,005	0,4247±0,013	0,4423±0,022	0,4523±0,013	0,4603±0,014	0,4480±0,005
	4	0,4380±0,005	0,4243±0,013	0,4297±0,026	0,4503±0,013	0,4443±0,018	0,4460±0,005
	4,5	0,4290±0,006	0,4233±0,013	0,4190±0,026	0,4483±0,013	0,4260±0,017	0,4440±0,004
	5	0,4200±0,007	0,4227±0,013	0,4100±0,03	0,4463±0,013	0,4123±0,019	0,4427±0,004
	5,5	0,4107±0,008	0,4213±0,012	0,4033±0,034	0,4440±0,012	0,4033±0,023	0,4413±0,004
	6	0,4020±0,008	0,4203±0,012	0,3973±0,039	0,4427±0,012	0,3953±0,024	0,4393±0,004

Using the absorbance values obtained, the activity of the GR enzyme was calculated. It is important to note that a unit of GR activity is defined as the amount of enzyme that catalyzes the reduction of 1µmol of GSSG per minute, or equivalently, oxidizes 1µmol of NADPH per minute. The change in absorbance at 340nm is proportional to the change in NADPH concentrations, as dictated by the Lambert-Beer law Mannervik (1999):

$$\Delta A = \varepsilon l \Delta c$$

Thus, the enzymatic activity per unit time (Δc) is determined by dividing the change in absorbance (ΔA) by the product of the molar extinction coefficient (ε=6.2mM^{-1}cm^{-1}) and the path length (l=1cm). The resulting values of enzymatic activity are presented in *Table 10*.

Table 10. Values of enzymatic activity of glutathione reductase per unit of time. *The activity has been calculated following the Lambert-Beer law ($\Delta A = \varepsilon l \Delta c$), where ε=6.2mM^{-1}cm^{-1} and l=1cm. The units of enzymatic activity are µM/min.*

	TIME (MIN)	TREATMENT					
		CONTROL		10% PEG		20% PEG	
		Stem	Roots	Stem	Roots	Stem	Roots
ENZYMATIC ACTIVITY (µM/MIN)	0,5	161,7204	137,0968	171,9355	146,9892	190,1075	151,0753
	1	77,4194	67,5806	83,0645	74,1935	90,2151	75,2151
	1,5	51,2545	45,0896	54,2294	49,2832	58,0645	49,6774
	2	37,9839	34,0591	39,4355	36,8011	41,9892	36,9892
	2,5	29,9140	27,3978	30,4946	29,3978	32,1505	29,4194
	3	24,4982	22,8674	24,5878	24,4265	25,7168	24,3190
	3,5	20,5991	19,5699	20,3840	20,8449	21,2135	20,6452
	4	17,6613	17,1102	17,3253	18,1586	17,9167	17,9839
	4,5	15,3763	15,1732	15,0179	16,0693	15,2688	15,9140
	5	13,5484	13,6344	13,2258	14,3978	13,3011	14,2796
	5,5	12,0430	12,3558	11,8280	13,0205	11,8280	12,9423
	6	10,8065	11,2993	10,6810	11,8996	10,6272	11,8100

In *Figure 13*, the decrease in GR enzyme activity for each sample over time is illustrated. Notably, the enzyme appears to be more abundant in the stem compared to the roots, following a similar pattern to other compounds. Similarly, it can be observed that water stress does not affect all parts of the plant uniformly. Furthermore, distinct effects are noticed with varying concentrations of PEG. For instance, in the case of the stem, administration of both 10% and 20% PEG solutions leads to an increase in GR activity, with the former exhibiting a more pronounced effect. Conversely, in the roots, water stress induced by the 10% PEG treatment significantly enhances GR activity. However, the activity in the control group exceeds that of plants treated with the 20% PEG solution.

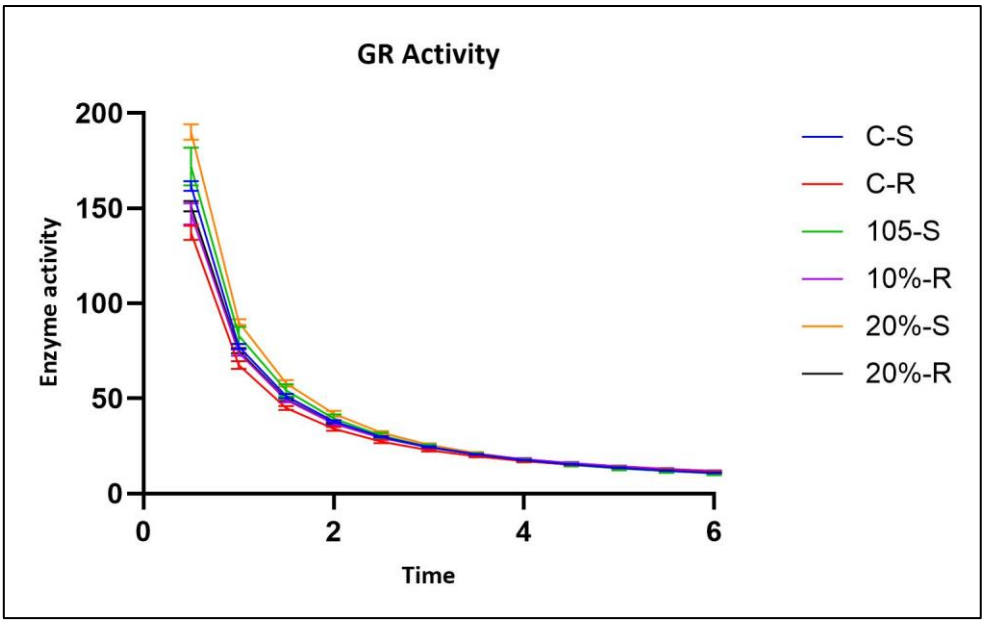

Figure 13. **Scatter plot of the glutathione reductase enzyme activity from different samples**. Enzymatic activity is measured in µM/min, and time units are in minutes.

5.5. The GSH:GSSG ratio increases with 10% PEG adminstration in both roots and stem.

To determine the glutathione content, fluorescence was measured (excitation 360nm/emission 460nm). A TCEP solution was used to quantify the total glutathione, including both the reduced (GSH) and oxidized (GSSG) forms, whereas the TRIS/HCl buffer was employed to measure only the GSH content. The results are presented in *Table 11*.

Table 11. Fluorescence values of the samples. Measurements were conducted at excitation 360nm/emission 460nm. The values obtained using TCEP solution correspond to the toTal glutathione content (sum of GSH and GSSG), while the values obtained using the TRIS/HCl buffer represent the GSH content only.

		TREATMENT					
		CONTROL		10% PEG		20% PEG	
		Stem	Roots	Stem	Roots	Stem	Roots
EXC 360/EM 460 NM	**TCEP reagent**	22140	22418	21303	23604	21759	24034
		22291	24054	22604	23537	22604	24627
		22727	22189	22990	23334	22978	23675
	Mean ± SD	22386±305	22887±1017	22299±884	23491,67±141	22447±624	24112±481
	Buffer	16277	13980	19275	17061	20277	15056
		16740	14505	19563	17373	19943	15127
		16777	14175	18057	17308	19375	14905
	Mean ± SD	16598±279	14220±265	18965±799	17247,33±165	19865±456	15029,33±113

Two calibration curves were established using GSH and GSSG standards, respectively. The calibration curve for the GSH standards was $y = 138{,}69x + 12730$ (R^2=0,9989), and the

calibration curve for the GSSG standard was $y = 2{,}7031x + 21985$ (R^2=0,9953). Using these calibration equations, the concentrations of total glutathione and GSH were calculated. The GSSG concentration was determined by subtracting the GSH value from the total glutathione value. Additionally, the GSH/GSSG ratio was calculated. The final concentrations of GSH and GSSG are presented in *Table 15*, with units µmol/l.

Table 15. GSH and GSSG content in the different samples. *Total glutathione concentrations were calculated using the calibration curve* $y = 2{,}7031x + 21985$ (R^2=0,9953)*, and GSH concentrations were calculated using the calibration curve* $y = 138{,}69x + 12730$ (R^2=0,9989)*. The GSSG concentration corresponds to the difference between the total glutathione and GSH concentrations.*

TREATMENT		[GSH] (µMOL/L)	[TOTAL GLUTATHIONE] (µMOL/L)	[GSSG] (µMOL/L)	RATIO ([GSH]/[GSSG])
CONTROL	Stem	27,8895±2,01	148,3482±112,76	120,4587±111,28	0,2315
	Roots	10,7434±1,91	333,6909±376,28	322,9476±374,59	0,0333
10% PEG	Stem	44,9564±5,76	116,1629±326,99	71,2065±330,10	0,6314
	Roots	32,5714±1,19	557,3847±52,01	524,8133±52,66	0,0621
20% PEG	Stem	51,4457±3,29	170,9149±231,02	119,4692±234,09	0,4306
	Roots	16,5789±0,82	786,8743±177,86	770,2954±177,09	0,0215

In *Figure 14*, the graphical representation of the GSH/GSSG ratio values is presented. Analogous to the other identified compounds, it can be observed that the different parts of the plant do not follow the same pattern. The highest ratio, both in the roots and the stem, corresponds to the samples treated with a 10% PEG solution. However, in the roots, a higher ratio was obtained in the control samples compared to the samples treated with a 20% PEG solution. While in the stem, the opposite situation was observed, with a higher ratio in the samples treated with a 20% PEG solution compared to the control samples.

Examining the individual concentrations of GSH and GSSG shown in *Table 15*, it can be seen that the distribution among the samples is slightly different. For GSH, the highest concentration is found in the control group, both in the roots and the stem. However, the case of GSSG is different; in the roots, the highest concentration is indeed found in the control group, but in the stem, it is found in the samples treated with the 10% PEG solution.

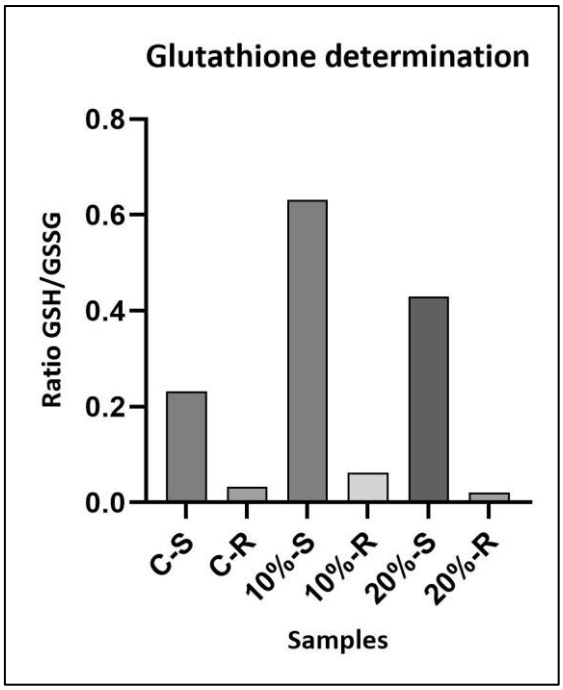

***Figure 14*. Bar chart depicting the GSH/GSSG ratio of the various samples.** *From left to right, the samples are as follows: stem control (C-S), root control (C-R), stem treated with 10% PEG solution (10%-S), roots treated with 10% PEG solution (10%-R), stem treated with 20% PEG solution (20%-S), and roots treated with 20% PEG solution (20%-R).*

6. DISCUSSION

As previously mentioned, there is scientific evidence indicating that various abiotic stresses can induce oxidative damage in plants by disrupting the balance between reactive oxygen species (ROS) production and the quenching activity of antioxidants (Hernández et al., 1999). Under these unfavorable conditions for plant growth and development, both the biosynthesis of antioxidant compounds and the activity of enzymes are altered (Tokarz et al., 2021). The presented results suggest a correlation between water stress during the early stages of *Pisum sativum L.* growth and the onset of oxidative stress.

The results obtained in this study corroborate the expectations, as shown in *Figure 11*, where MDA levels increase with the administered PEG concentration. It is noteworthy that the increase in MDA concentrations is more pronounced in the stem compared to the roots, where MDA levels exhibit low variation.

Previous studies assessing the effect of different environmental stresses on *Pisum sativum L.* have obtained similar results, confirming an increase in ROS and consequent oxidative damage.

Dixit et al. investigated the effect of Cd administration on pea roots and stems, observing a greater increase in MDA concentrations in the roots compared to the leaves. This suggests that the plant's response to ionic stress differs from its response to water stress.

On the other hand, *Hernández et al.* observed a significant increase in MDA concentrations in plants subjected to 8 hours of saline stress, although they noted a rapid decrease in the following hours, suggesting potential adaptation to the stress conditions. This raises the possibility that plants may also adapt to water stress if subjected to it for a prolonged period. In the same study, they found no strong osmotic stress during the short period of saline stress, concluding that the increase in MDA could be due to the toxic effects of salts rather than osmotic stress. Thus, considering the results obtained in previous studies and the present one, it can be suggested that different environmental stresses induce oxidative stress, despite the plant's response is not always consistent and depends on the level and duration of stress to which they are subjected.

To mitigate the oxidative stress induced by water stress, the intricate antioxidative mechanisms of plants come into play, comprising various enzymes and compounds. In this study, as previously elucidated, our investigation centers on discerning alterations in the activity of the enzyme GR, responsible for catalyzing the reduction of GSSG, and changes in glutathione concentrations, specifically its reduced and oxidized forms, given its pivotal role in maintaining cellular redox homeostasis.

It is to be expected that under environmental stress, oxidative damage would escalate. In a study conducted by *Hernández et al.*, which aimed to characterize the antioxidative response of *Pisum sativum L.* subjected to NaCl-induced stress, severe stress led to a gradual decline in the GSH/GSSG ratio, resulting in GSSG accumulation. It was concluded that the induced activity of the GR enzyme in stressed plants proved insufficient to maintain the GSH pool, implying a potential restriction of glutathione synthesis due to elevated NaCl concentrations.

Conversely, *Dixit et al.* observed a decrement in GSH concentrations following plant exposure to Cd, although without significant changes in GSSG levels compared to the control. Additionally, the monitoring of GR enzyme activity revealed a noteworthy augmentation on the initial day of treatment, despite subsequently diminishing below control levels in the following days.

It is notable that prior studies have already suggested the crucial role of the GR enzyme in combating oxidative stress in plants. However, its activity has been shown to vary depending on the plant species and the types of stress it undergoes. For instance, in stress induced by metallic ions, *Gallego et al.*, *Chaoui et al.*, and *Shickler et al.* observed that Zn and Ni stimulated GR activity, while Cu and Fe has the opposite effect, diminishing it. Moreover, other studies noted that Cd induces an increase in GR activity in the genus *Allysum*, while decreasing activity in the genus *Helianthus annuus*.

Observing the results obtained in the present study, it is plausible to suggest that water stress potentiated GR enzyme activity, as evidenced by the GSH concentrations obtained, which did not decrease as expected. Furthermore, different behaviors between the stem and roots were observed, likely due to the comparison of two functionally distinct plant organs. Roots, being non-photosynthetic tissue, may experience relatively low ROS flux compared to the stem, where there is active electron transport.

Considering previous studies, it is conceivable to suggest the possibility of adaptation of GR enzyme to the presence of water stress, potentially explaining the slight increase in its activity during the extended stress period. As its behavior in the initial hours of stress is not yet fully understood, studying enzyme activity and determining glutathione content could offer insights into how these parameters change over time.

It is well-established that nitric oxide, in the presence of oxygen, can engage in a reaction with GSH to yield S-nitrosoglutathione (GSNO), a reactive nitrogen species serving as a signaling molecule capable of traversing organelles, neighboring cells, and propagating throughout the plant (Romero-Puertas et al., 2006).

Barroso et al. focused on studying the localization of GSNO and the expression of S-nitrosoglutathione reductase (GSNOR) in peas subjected to Cd stress. While many studies related to GSNO have been conducted in animal cells, where it is considered a natural reservoir of NO^+, in plants, it had only been hypothesized as a molecule involve in NO^+ signaling pathways. In their work, it was discovered that Cd stress down-regulated both the activity and expression of GSNOR, likely due to a decrease in GSNO formation, which is its substrate. Previously, it had been demonstrated that Cd induces oxidative stress in peas (Sandalio et al., 2001), but their results indicated that it was highly unlikely to also cause nitrosative stress, suggesting that oxidative stress and nitrosative stress are not necessarily related.

In the present study, quantification of S-nitrosothiol (SNO) levels, a primary class of reactive nitrogen species generated through NO-mediated covalent modifications of thiol groups, was undertaken. As illustrated in *Figure 12,* overall, water stress causes an increase in SNO content, although a regular pattern cannot be discerned. Thus, it could be suggested that, similarly to the experiment conducted by *Barroso et al.*, there is not a complete correlation between oxidative stress and nitrosative stress induced by the water stress experienced by the peas. Nevertheless, further investigation is warranted to better localize and characterize the presence of GSNO and other S-nitrosothiols, and to study the activity of the GSNOR enzyme in peas subjected to water stress, in order to arrive at a valid conclusion.

7. CONCLUSIONS

The aim of this study was to investigate how stress induced by water deficit and osmotic stress affects the antioxidant mechanisms related to glutathione in *Pisum sativum L.*

In conclusion, it has been demonstrated that water stress is accompanied by oxidative stress, as evidenced by increased lipid peroxidation in both roots and stems as the concentration of PEG rises.

However, the results regarding glutathione levels and glutathione reductase activity are inconclusive. One would expect a decrease in the GSH/GSSG ratio due to the oxidative environment generated in cells in response to increased ROS. However, an increase in GSH concentrations has been observed, along with generally irregular behavior, complicating the extraction of clear conclusions.

Regarding GR activity, it has been noted that its activity is enhanced in plants treated with 20% PEG solution, which aligns with expectations as the plant seeks to restore the appropriate cellular redox environment.

Regarding SNO, clear results were also not obtained. An increase in their concentrations was expected due to the elevated levels of NO during induced stress, however, the results did not show a correlation between the percentage of PEG administered and the concentrations of SNO obtained.

Overall, considering the results of this study alongside those of previous studies, it can be suggested that various environmental factors can induce stress in plants, accompanied by oxidative stress. Nevertheless, plant responses and defense mechanisms may vary, contingent upon the level and duration of stress they are subjected to.

8. REFERENCES

Alché, J. de D. (2019). A concise appraisal of lipid oxidation and lipoxidation in higher plants. In *Redox Biology* (Vol. 23). Elsevier B.V. https://doi.org/10.1016/j.redox.2019.101136

Anderson, M. T., Trudell, J. R., Voehringer, D. W., Tjioe, I. M., & Herzenberg, L. A. (1999). *NOTES & TIPS An Improved Monobromobimane Assay for Glutathione Utilizing Tris-(2-carboxyethyl)phosphine as the Reductant*. http://www.idealibrary.com

Ashraf, M. A., Rasheed, R., Rizwan, M., Hussain, I., Aslam, R., Qureshi, F. F., Hafiza, B. S., Bashir, R., & Ali, S. (2023). Effect of exogenous taurine on pea (Pisum sativum L.) plants under salinity and iron deficiency stress. *Environmental Research*, *223*. https://doi.org/10.1016/j.envres.2023.115448

Gow, A., Doctor, A., Mannick, J., & Gaston, B. (2007). S-Nitrosothiol measurements in biological systems. In *Journal of Chromatography B: Analytical Technologies in the Biomedical and Life Sciences* (Vol. 851, Issues 1–2, pp. 140–151). https://doi.org/10.1016/j.jchromb.2007.01.052

Hernández, J. A., & Almansa, M. S. (2002). Short-term effects of salt stress on antioxidant systems and leaf water relations of pea leaves. *Physiologia Plantarum*, *115*(2), 251–257. https://doi.org/10.1034/j.1399-3054.2002.1150211.x

Hernández, J. A., Campillo, A., Jiménez, A., Alarcón, J. J., & Sevilla, F. (1999). Response of antioxidant systems and leaf water relations to NaCl stress in pea plants. *New Phytologist*, *141*(2), 241–251. https://doi.org/10.1046/j.1469-8137.1999.00341.x

Hodges, D. M., DeLong, J. M., Forney, C. F., & Prange, R. K. (1999). Improving the thiobarbituric acid-reactive-substances assay for estimating lipid peroxidation in plant tissues containing anthocyanin and other interfering compounds. *Planta*, *207*(4), 604–611. https://doi.org/10.1007/s004250050524

Lahuta, L. B., Szablińska-Piernik, J., & Horbowicz, M. (2022). Changes in Metabolic Profiles of Pea (Pisum sativum L.) as a Result of Repeated Short-Term Soil Drought and Subsequent Re-Watering. *International Journal of Molecular Sciences*, *23*(3). https://doi.org/10.3390/ijms23031704

Lu, Z. X., He, J. F., Zhang, Y. C., & Bing, D. J. (2020). Composition, physicochemical properties of pea protein and its application in functional foods. In *Critical Reviews in Food Science and Nutrition* (Vol. 60, Issue 15, pp. 2593–2605). Taylor and Francis Inc. https://doi.org/10.1080/10408398.2019.1651248

Mangal, V., Lal, M. K., Tiwari, R. K., Altaf, M. A., Sood, S., Gahlaut, V., Bhatt, A., Thakur, A. K., Kumar, R., Bhardwaj, V., Kumar, V., Singh, B., Singh, R., & Kumar, D. (2023). A comprehensive and conceptual overview of omics-based approaches for enhancing the resilience of vegetable crops against abiotic stresses. In *Planta* (Vol. 257, Issue 4). Springer Science and Business Media Deutschland GmbH. https://doi.org/10.1007/s00425-023-04111-5

Mannervik, B. (1999). Measurement of Glutathione Reductase Activity. *Current Protocols in Toxicology*, *00*(1). https://doi.org/10.1002/0471140856.tx0702s00

Mittova, V., Theodoulou, F. L., Kiddle, G., Gómez, L., Volokita, M., Tal, M., Foyer, C. H., & Guy, M. (2003). Coordinate induction of glutathione biosynthesis and glutathione- metabolizing

enzymes is correlated with salt tolerance in tomato. *FEBS Letters*, *554*(3), 417–421. https://doi.org/10.1016/S0014-5793(03)01214-6

Noctor, G., Mhamdi, A., Chaouch, S., Han, Y., Neukermans, J., Marquez-Garcia, B., Queval, G., & Foyer, C. H. (2012). Glutathione in plants: An integrated overview. *Plant, Cell and Environment*, *35*(2), 454–484. https://doi.org/10.1111/j.1365-3040.2011.02400.x

Piterková, J., Luhová, L., Zajoncová, L., Šebela, M., & Petřivalský, M. (2012). Modulation of polyamine catabolism in pea seedlings by calcium during salinity stress. *Plant Protection Science*, *48*(2), 53–64. https://doi.org/10.17221/62/2011-pps

Popović, B. M., Štajner, D., Ždero-Pavlović, R., Tari, I., Csiszár, J., Gallé, Poór, P., Galović, V., Trudić, B., & Orlović, S. (2017). Biochemical response of hybrid black poplar tissue culture (Populus × canadensis) on water stress. *Journal of Plant Research*, *130*(3), 559–570. https://doi.org/10.1007/s10265-017-0918-4

Romero-Puertas, M. C., Corpas, F. J., Sandalio, L. M., Leterrier, M., Rodriguez-Serrano, M., del Rio, L. A., & Palma, J. M. (2006). Glutathione reductase from pea leaves: response to abiotic stress and characterization of the peroxisomal isozyme. *New Phytologist*, *170*(1), 43–52. https://doi.org/10.1111/j.1469-8137.2005.01643.x

Sandalio, L. M., Dalurzo, H. C., Gó Mez, M., Romero-Puertas, M. C., & Del Río, L. A. (n.d.). *Cadmium-induced changes in the growth and oxidative metabolism of pea plants*.

Soudek, P., Langhansová, L., Dvořáková, M., Revutska, A., Petrová, Š., Hirnerová, A., Bouček, J., Trakal, L., Hošek, P., & Soukupová, M. (2024). The impact of the application of compochar on soil moisture, stress, yield and nutritional properties of legumes under drought stress. *Science of The Total Environment*, *914*, 169914. https://doi.org/10.1016/j.scitotenv.2024.169914

Szablińska-Piernik, J., & Lahuta, L. B. (2021). Metabolite profiling of semi-leafless pea (Pisum sativum L.) under progressive soil drought and subsequent re-watering. *Journal of Plant Physiology*, *256*. https://doi.org/10.1016/j.jplph.2020.153314

Tokarz, K. M., Wesołowski, W., Tokarz, B., Makowski, W., Wysocka, A., Jędrzejczyk, R. J., Chrabaszcz, K., Malek, K., & Kostecka-Gugała, A. (2021). Stem photosynthesis—a key element of grass pea (Lathyrus sativus l.) acclimatisation to salinity. *International Journal of Molecular Sciences*, *22*(2), 1–33. https://doi.org/10.3390/ijms22020685

Zor, T., & Selinger, Z. (1996). Linearization of the Bradford Protein Assay Increases Its Sensitivity: Theoretical and Experimental Studies. In *ANALYTICAL BIOCHEMISTRY* (Vol. 236).

Note: Some translations from spanish to english in this document were done using OpenAI. (2024). *ChatGPT (September 2024)* [Large language model]. OpenAI. https://www.openai.com/